Structural Analysis Locates Aplaviroc in the Interface of ECL and TM Domains—In the present study, a three-dimensional model of human CCR5-CCR5 inhibitor complex was defined by combining the results of site-directed mutagenesis-based analyses (Table 1) and molecular modeling that involved structure refinement and simultaneous docking of inhibitors to an initial structure of CCR5 based on the crystal structure of bovine rhodopsin (23). Fig. 2 illustrates the three-dimensional model of CCR5 that has a seven-transmembrane helical structure. Six hydrophobic cavities were identified in the extracellular, transmembrane, and intracellular domains of CCR5. Among them, a hydrophobic cavity to which CCR5 inhibitors highly likely to bind was identified based on its size and location (*red arrowhead* in Fig. 2). This cavity is the largest one among the six that can accommodate a molecule of the size of AVC and other CCR5 inhibitors and is in the region implicated to have the greatest effect on K_D values with amino acid substitutions introduced in CCR5 among the six hydrophobic cavities identified. It should be noted, however, that the conformations of CCR5 without an inhibitor and CCR5 with the inhibitor can be substantially different from each other, because significant conformational changes would be expected to follow ligand binding to CCR5. Nevertheless, it is intriguing to note that this largest cavity corresponds to the binding site for the retinal ligand in bovine rhodopsin; given the propensity of this pocket to bind fairly large ligands such as the CCR5 inhibitors, it is possible that this binding cavity could accommodate some as-yet uncharacterized ligands produced in the body during the normal function of CCR5, potentially even some with regulatory roles.

FIGURE 2. **Hydrophobic cavities identified within CCR5.** Six hydrophobic cavities are identified within human CCR5, defined using MOLCAD (Sybyl 7.0). Note the largest hydrophobic cavity (*red arrowhead*) that is likely to accommodate a molecule of the size of AVC and other CCR5 inhibitors and is in the region implicated to have greatest effects on K_D values (see mutagenesis-based results in Table 1).

Based on the set of the K_D values of AVC in relation to various mutant CCR5 species overexpressed on CHO cells (Table 1), structural analysis of AVC-CCR5 interactions was conducted, which suggested that a series of intramolecular and intermolecular hydrogen bonds occur, which should stabilize the CCR5-AVC complex. We identified a significant network of hydrogen bonds among four amino acid residues: Gly^{163}, Ser^{180}, Lys^{191}, and Thr^{195} (Fig. 3*A*). Gly^{163} is located in TM4, Ser^{180} in ECL2, and Lys^{191} and Thr^{195} in TM5. Another network of hydrogen bonds was identified among another four amino acid residues: Tyr^{37}, Glu^{283}, Met^{287}, and Tyr^{108} (Fig. 3*B*). Tyr^{37} is located in TM1, Tyr^{108} in TM3, and Glu^{283} and Met^{287} in TM7. These hydrogen bond networks spanning multiple domains appear to maintain the optimal shape of the cavity for the binding of AVC. Indeed, further analysis of the cavity also revealed that the ECL regions have some hydrophilic characters (Fig. 4*A*, *red arrowhead*), whereas the rest of the cavity is mostly lipophilic (Fig. 4*A*). The carboxyl and hydroxymethyl of AVC interact with the hydrophilic regions of CCR5. The rest of AVC inter-

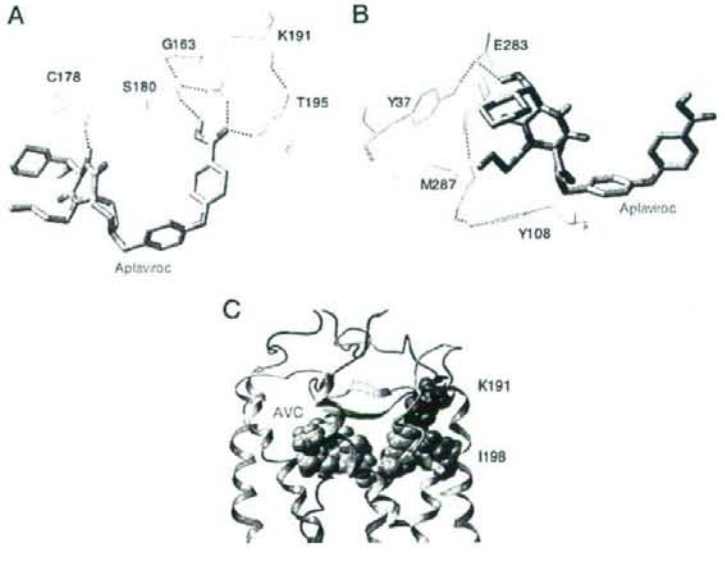

FIGURE 3. **Hydrogen bond networks within CCR5 critical for AVC binding to CCR5.** The structure of the CCR5-AVC complex was defined with iterative structural refinement using docking and homology modeling. Only polar hydrogen atoms are shown. *Panel A*, an intramolecular hydrogen bond network comprised of Gly^{163}, Ser^{180}, Lys^{191}, and Thr^{195} is seen. Gly^{163} is located in TM4, Ser^{180} in ECL2, and Lys^{191} and Thr^{195} in TM5. The structural analyses illustrate the presence of intermolecular hydrogen bonds of AVC with residues Cys^{178}, Ser^{180}, Lys^{191}, and Thr^{195} of CCR5. *Panel B*, an intramolecular hydrogen bond network is seen involving Tyr^{37}, Glu^{283}, Met^{287}, and Tyr^{108}. Tyr^{37} is located in TM1, Tyr^{108} in TM3, and Glu^{283} and Met^{287} in TM7. Glu^{283} forms hydrogen bond interactions with the hydroxymethyl of AVC. Intramolecular hydrogen bonds are shown in *pink*, and the intermolecular hydrogen bonds in *green*. Note that the hydrogen bond networks spanning multiple domains should maintain the optimal shape of the cavity for the binding of AVC (Fig. 4, *A* and *B*). *Panel C*, the predicted van der Waals contact between AVC and CCR5 residues Lys^{191} and Ile^{198}. AVC is shown in *green spheres*, whereas Lys^{191} and Ile^{198} in *magenta*.

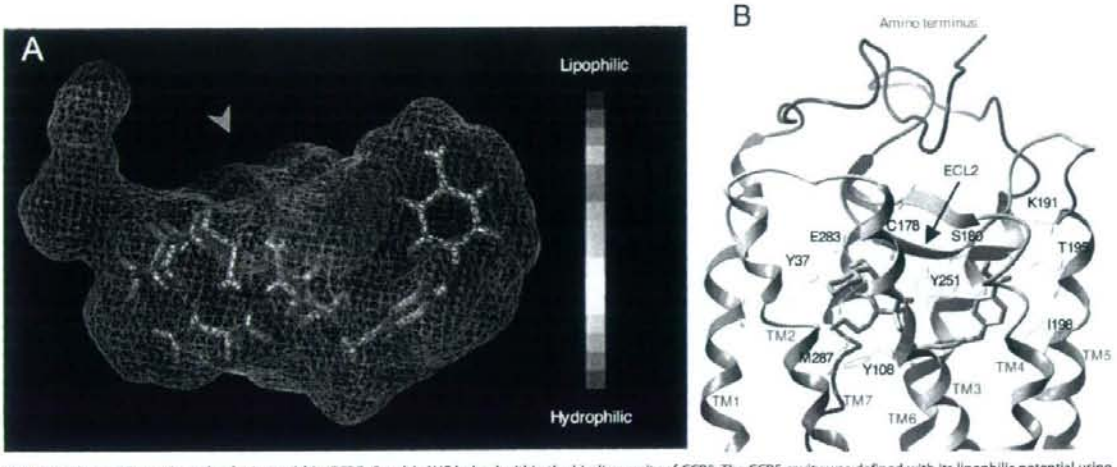

FIGURE 4. **The configuration of aplaviroc within CCR5.** *Panel A*, AVC lodged within the binding cavity of CCR5. The CCR5 cavity was defined with its lipophilic potential using MOLCAD. The region near the extracellular domain has some hydrophilic character (*red arrowhead*), whereas the rest of the cavity is mostly lipophilic. The carboxyl and hydroxymethyl of AVC interact with the hydrophilic regions of CCR5, whereas the rest of AVC interacts with the lipophilic regions of CCR5. *Panel B*, a docked structure of AVC (tube representation) bound to CCR5, illustrating the relative location of AVC within CCR5. Important binding site residues of CCR5 are shown in *wires*. Polar hydrogens are only shown. Note that TM1, 2, and 3 are toward the viewer from the plane and TM6 and 7 are away from the viewer behind the plane.

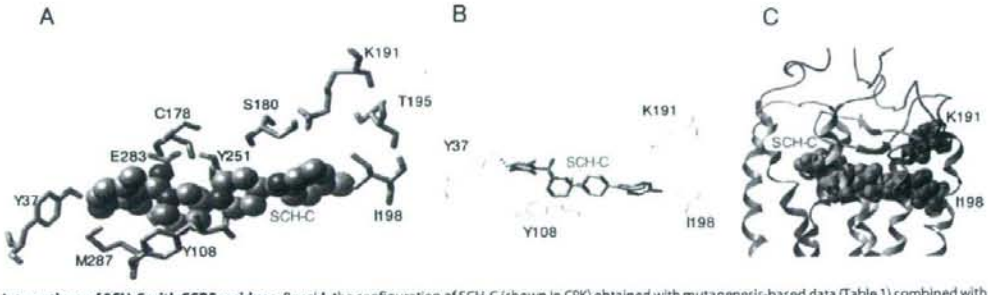

FIGURE 5. **Interactions of SCH-C with CCR5 residues.** *Panel A*, the configuration of SCH-C (shown in CPK) obtained with mutagenesis-based data (Table 1) combined with structural analyses. CCR5 residue orientations (shown in *tubes*) vary from that in Fig. 4 because conformational flexibility of receptors during docking of each inhibitor was taken into account. *Panel B*, Tyr^{37} forms hydrogen bonding interactions with SCH-C, and hence Y37A mutation reduces the binding affinity of SCH-C with CCR5. Note the location of Tyr^{108} and compare its corresponding location for the complex with TAK-779. SCH-C is shown in *tubes* and CCR5 residues in *wires*. Only polar hydrogens are shown in *panels A* and *B*. The molecules are colored by atom types (carbon, *gray*; oxygen, *red*; nitrogen, *blue*; hydrogen, *cyan*; sulfur, *yellow*; and bromine, *green*). *Panel C*, van der Waals interactions of SCH-C (*green*) with Lys^{191} and Ile^{198} (*magenta*). There is tight hydrophobic binding of SCH-C with Ile^{198}. Unlike AVC, Lys^{191} does not form significant interactions with SCH-C.

acts with the lipophilic region of CCR5 (Fig. 4, *A* and *B*). It is of note that AVC has a molecular weight of 614.2, larger than TAK-779 (M_r 531.1) and SCH-C (M_r 557.5), has a substantial hydrophobic contact and fits well inside the large binding cavity within CCR5 as shown in Fig. 4*A*. AVC also forms hydrogen bonds with Cys^{178}, Ser^{180}, Lys^{191}, and Thr^{195} (Fig. 3, *A* and *B*). It is presumed that these interactions with residues in multiple ECLs and the interface of extracellular and transmembrane domains are responsible for the tight binding of AVC to CCR5.

Amino Acid Substitutions Are Likely to Cause Substantial Conformational Changes in ECLs—Substitutions of amino acid residues, which are involved in hydrogen bonding, appear to directly and indirectly disrupt the hydrogen bond networks observed (Fig. 3, *A* and *B*). For example, Gly^{163}, located in TM4, does not interact directly with AVC, but is responsible for maintaining the shape of the binding cavity by its hydrogen bond interactions with Ser^{180} and Lys^{191} (Fig. 3*A*). Thus, the shape of the cavity is most likely altered with G163R substitution, and thereby AVC could lose critical interactions with ECL2 and TM5. In contrast, it was found that G163R exerts minimal effects on the binding of either SCH-C or TAK-779 to CCR5 (Table 1), potentially because these two inhibitors do not have direct hydrogen bond interactions with the ECL or ECL-TM interface.

As mentioned above, the carboxyl of AVC forms hydrogen bonds with Lys^{191} and Ser^{180} (Fig. 3*A*). The loss of binding with K191A substitution (Table 1) is likely because of the loss of the hydrogen bond with AVC as well as the altered shape of the cavity, which was confirmed by structural analysis of the $CCR5_{K191A}$-AVC complex. Neither SCH-C nor TAK-779 forms hydrogen bonds with Lys^{191} (Fig. 5, *A* and *B*, and Fig. 6*A*), hence it is thought that K191A substitution does not significantly affect the binding affinity of SCH-C or TAK-779 (Table 1). Ile^{198} located in TM5 has hydrophobic interactions with AVC (Fig. 3*C*). SCH-C and TAK-779 were predicted to have hydrogen bond interactions with Tyr^{37} located in TM1 (Fig. 5, *A* and *B*, and Fig. 6, *A* and *B*), whereas there appear to be no such interactions with AVC (Fig. 3*B*). This is consistent with the observation that Y37A substitution drastically changed the binding affinity of SCH-C and TAK-779 to CCR5 (Table 1). Ile^{198} forms a hydrophobic contact with SCH-C (Fig. 5*C*), although not much with TAK-779, which well explains the reason I198A reduces the K_D value of SCH-C with CCR5 but not that of TAK-

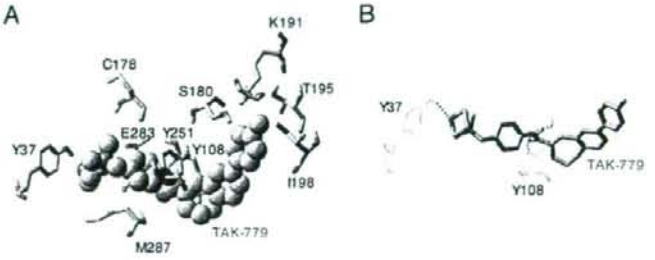

FIGURE 6. **Interactions of TAK-779 with CCR5 residues.** *Panel A*, the configuration of TAK-779 within the CCR5 binding pocket. *Panel B*, Tyr^{37} forms a hydrogen bonding interaction with TAK-779. Note the orientation of Tyr^{108} in comparison to the complex of CCR5 with SCH-C. Tyr^{108} forms π-π and hydrogen bond interactions with TAK-779 and represents a critical residue in agreement with the mutagenesis-based results (Table 1). Only polar hydrogens are shown. The molecules are colored by atom types (carbon, *gray*; oxygen, *red*; nitrogen, *blue*; hydrogen, *cyan*; sulfur, *yellow*).

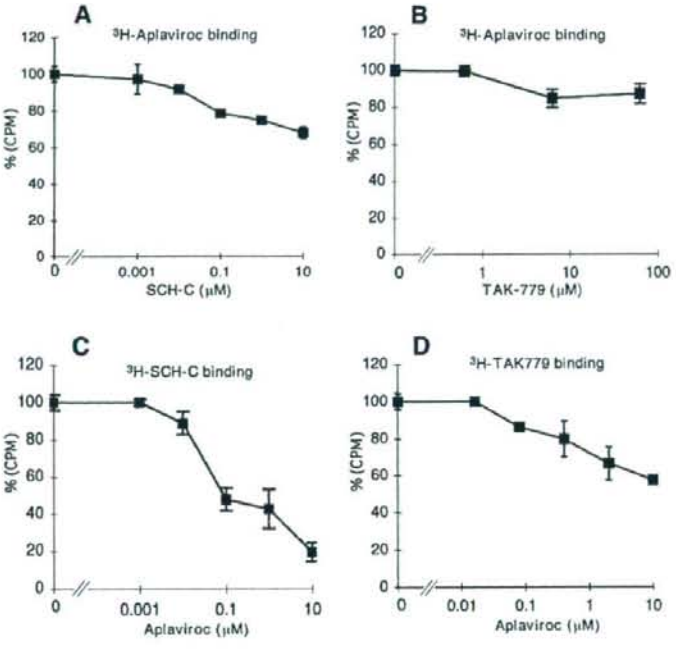

FIGURE 7. **Interactions between CCR5 inhibitors in relation to CCR5.** $CCR5_{WT}$-CHO cells were exposed to [^{3}H]AVC (3 nM; *panels A* and *B*), [^{3}H]SCH-C (3 nM; *panel C*), or [^{3}H]TAK-779 (10 nM; *panel D*), for 15 min, followed by the exposure to various concentrations (from 1 nM to 62.5 μM) of unlabeled SCH-C (*panel A*), TAK-779 (*panel B*), or AVC (*panels C* and *D*) for 30 min. The cells were then thoroughly washed, lysed, and the radioactivity of the lysates counted. All experiments were performed in duplicate and the data shown are mean values ± S.D. The amounts of the [^{3}H]CCR5 inhibitor bound to the cells are shown as mean % control values (each control value was obtained without an indicated unlabeled CCR5 inhibitor).

779 with CCR5 (Table 1). It is also of note that AVC has direct interactions with residues in the extracellular domain and its proximity (Cys^{178}, Ser^{180}, and Lys^{191}) (Fig. 3, *A* and *B*), which should strongly affect the conformation of extracellular loops in comparison to SCH-C and TAK-779, both of which failed to directly interact with the amino acid residues in the extracellular domain. The interaction of HIV-1-gp120 with ECLs is thought to be critical for the establishment of infection, therefore, one can assume that the binding of AVC to CCR5 should result in a significant loss of interactions with gp120, which could explain the significantly greater effect of AVC in blocking viral infectivity, compared with SCH-C and TAK-779. Thus, the data above suggest that the binding pockets are in the same general area within CCR5, however, the binding interactions of the three inhibitors with CCR5 residues substantially differ from each other, in particular between AVC and other two inhibitors.

Interactions between CCR5 Inhibitors in Relation to Their Binding to CCR5—All three CCR5 inhibitors examined in this study possess the properties of allosteric antagonists of CCR5, whereas AVC exerts only partial inhibition of the binding to CCR5 and physiological function of ^{125}I-RANTES in comparison to TAK-779 and SCH-C (11). Moreover, although the binding pocket for these inhibitors are all located in the same hydrophobic cavity within CCR5, their binding profiles substantially differ from each other as discussed above. Therefore, we analyzed the interactions of the three inhibitors in relation to $CCR5_{WT}$. When $CCR5_{WT}$-CHO cells were exposed to [^{3}H]AVC (3 nM) for 15 min, followed by the addition of various concentrations (1 nM to 10 μM) of unlabeled SCH-C, [^{3}H]AVC binding to CCR5 was reduced only moderately, by up to 32% (Fig. 7*A*). When the interaction between [^{3}H]AVC and unlabeled TAK-779 (0.625-62.5 μM) was examined, [^{3}H]AVC binding to CCR5 was not significantly replaced by unlabeled TAK-779 (Fig. 7*B*). On the contrary, when [^{3}H]SCH-C was added first and then unlabeled AVC was added, the binding of [^{3}H]SCH-C to $CCR5_{WT}$-CHO cells was significantly blocked (Fig. 7*C*). These data suggest that AVC effectively replaces [^{3}H]SCH-C and binds to $CCR5_{WT}$. The binding of [^{3}H]TAK-779 was likewise blocked by the addition of unlabeled AVC, although the extent of replacement by AVC was lesser as compared with the case of [^{3}H]SCH-C (Fig. 7*D*).

Role of Amino Acid Residues of CCR5 with Which Aplaviroc Is Associated in HIV-1 Infection and CC-chemokine Binding—In an attempt to define the biological and virological roles of amino acid residues, with which AVC is associated in this binding to CCR5, we selected 15 mutant CCR5-overexpressing CHO cells and examined profiles of sCD4/gp120

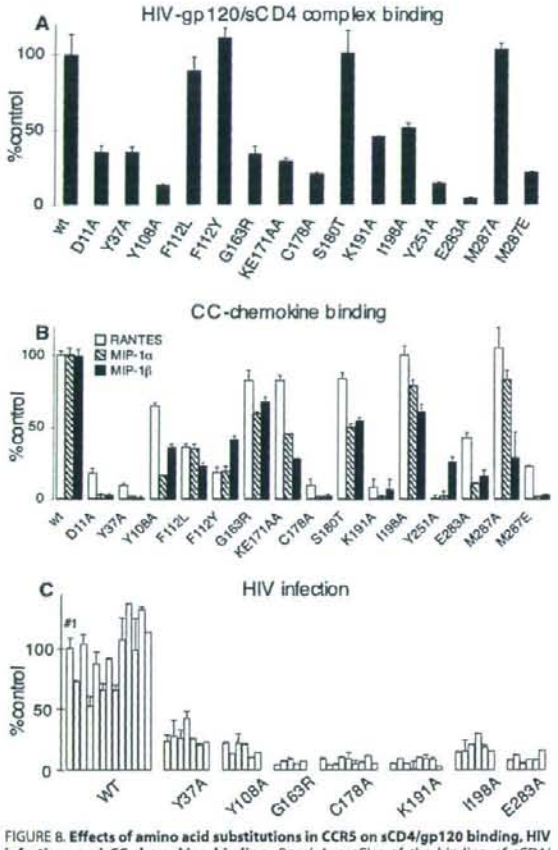

FIGURE 8. **Effects of amino acid substitutions in CCR5 on sCD4/gp120 binding, HIV infection, and CC-chemokine binding.** *Panel A*, profiles of the binding of sCD4/$gp120_{YU2}$ complex to various $CCR5_{MT}$ species overexpressing CHO cells. All values were normalized with the CCR5 expression level of each $CCR5_{MT}$ compared with that of $CCR5_{WT}$ (see "Experimental Procedures"). *Panel B*, profiles of the binding of ^{125}I-RANTES, ^{125}I-MIP-1α, and ^{125}I-MIP-1β to various $CCR5_{MT}$-expressing CHO cell preparations. All values were normalized with the CCR5 expression level of each $CCR5_{MT}$ compared with that of $CCR5_{WT}$. All assays were performed in duplicate or triplicate. *Panel C*, the susceptibility of various $CCR5_{MT}$-overexpressing U373-MAGI cells. For testing each $CCR5_{MT}$-overexpressing cell preparation, multiple clones were examined. In each set of experiments, $CCR5_{WT}$-clone 1 (*solid column*) served as a standard (100%).

binding and CC-chemokine (RANTES, MIP-1α, and MIP-1β) binding profiles. Nine of the 15 mutants were chosen based on the following reasons. Tyr^{108} was chosen because Tyr^{108} is within the aromatic cluster seen in the proximity of TM2 and TM3 and is reported to play a crucial role in the CC-chemokine-elicited activation of CCR5 (35). Y37A and E283A were chosen because Tyr^{37} and Glu^{283} are involved in the binding of the three inhibitors to CCR5 and have been shown to be highly conserved in CC-chemokine receptors including CCR5, CCR2B, CCR3, CCR1, and CCR4 (6). Six more mutants (G163R, C178A, K191A, I198A, Y251A, and M287E) were also chosen, with which the binding affinity of AVC was significantly reduced compared with $CCR5_{WT}$-expressing cells (>5-fold K_D difference) (Table 1). As shown in Fig. 8*A*, all 9 mutations described above decreased the sCD4/gp120 binding to CCR5 compared with that to $CCR5_{WT}$. It was noted that Y108A, Y251A, and E283A substitutions resulted in the greatest reduction of sCD4/gp120 binding.

We further determined the binding profiles of ^{125}I-RANTES, ^{125}I-MIP-1α, and ^{125}I-MIP-1β to the above 9 mutant CCR5-overexpressing CHO cell lines (Fig. 8*B*). In several CHO cell lines, the CC-chemokine binding profile notably differed from the HIV-gp120/sCD4 complex binding profile. Whereas both K191A and I198A substitutions caused moderate reduction in HIV-gp120/sCD4 complex binding (Fig. 8*A*), CC-chemokine binding was fairly preserved in $CCR5_{I198A}$-expressing cells, whereas CC-chemokine binding was almost completely reduced in $CCR5_{K191A}$-expressing cells. The G163R substitution preserved HIV-gp120/sCD4 complex binding by 34%, however, CC-chemokine binding was substantially spared by 68–83%.

We also employed six additional mutant CCR5-overexpressing CHO cells, which showed insignificant to minimal changes (less than 3-fold differences) in their K_D values compared with the K_D value for wild-type CCR5 (Table 1). Two substitutions in the extracellular domain of CCR5, D11A (NH_2 terminus) and KE171AA (ECL2), induced substantial reduction in HIV-gp120/sCD4 complex binding by 65 and 70%, respectively. The F112L, F112Y (both in TM3), S180T (ECL2), and M287A (TM7) substitutions caused no significant changes in K_D values (Table 1) or HIV-gp120/sCD4 complex binding (Fig. 8*A*). These data suggest that amino acid residues in the proximity of the hydrophobic cavity for AVC that do not change K_D values generally do not affect the HIV-gp120/sCD4 complex binding to CCR5. These 6 substitutions, however, caused CC-chemokine binding inhibition at various degrees, suggesting that the profile of the HIV-gp120/sCD4 complex binding to CCR5 differs from that of CC-chemokine binding to CCR5.

We finally generated seven clonal populations of $CD4^+$U373-MAGI cells expressing CCR5 with an amino acid substitution that caused significant reduction in the K_D values of either of the three CCR5 inhibitors and examined their susceptibility to HIV-1_{Bal} infection (Fig. 8*C*). HIV-1_{Bal} effectively infected $CCR5_{WT}$-expressing cells, however, the susceptibility to HIV-1_{Bal} infection was greatly reduced in $CCR5_{Y37A}$-, $CCR5_{Y108A}$-, and $CCR5_{I198A}$-expressing cells and that in $CCR5_{G163R}$-, $CCR5_{C178A}$-, $CCR5_{K191A}$-, and $CCR5_{E283A}$-expressing cells was more greatly limited. These data indicate that the mutations examined in this experiment effectively blocked HIV-1_{Bal} infection, although such mutations, in particular three mutations (G163R, K191A, and I198A), allowed some degree of sCD4/gp120 binding to $CCR5^+$ cells (Fig. 8*A*).

As noted above, the CC-chemokine binding profile notably differed from the profile of HIV-1_{Bal} infection susceptibility in $CCR5_{G163R}$- and $CCR5_{I198A}$-expressing cells. Moreover, moderate levels of chemokine binding were seen in $CCR5_{Y108A}$- and $CCR5_{E283A}$-expressing cells, whereas the least infection occurred in these cells. It should be of note that when we examined what ensued upon the binding of RANTES to $CCR5_{G163R}$-expressing cells, it was found that the level of Ca^{2+} flux that occurred in those cells was comparable with that in $CCR5_{WT}$-expressing cells following stimulation with RANTES.[3]

These data, taken together, suggest that the binding affinity of AVC seen with CCR5 variants generally paralleled the HIV-gp120/sCD4 complex binding affinity to mutant CCR5s, although it is of note that further fine-tuned analysis with greater numbers of CCR5 mutants is required for full understanding of the interactions among the HIV-gp120/sCD4 complex, CC-chemokines, and CCR5 inhibitors. The data also suggest that certain conformational changes caused by amino acid substitutions (*e.g.* at Tyr^{108}, Gly^{163}, or Ile^{198} residues of CCR5) might substantially reduce HIV-1 infection without significantly affecting physiological CC-chemokine-CCR5 interactions.

[3] K. Maeda, H. Nakata, T. Miyakawa, and H. Mitsuya, unpublished data.

DISCUSSION

In the present study, we examined the structural and molecular interactions between CCR5 and three CCR5 inhibitors, AVC, SCH-C and TAK-779. When we exploited site-directed mutagenesis by generating a panel of mutant CCR5-expressing cells, and determined the K_D values of each CCR5 inhibitor with each mutant CCR5 species, the K_D values compiled corroborated our previous results obtained using the mAb replacement assay (11). We found that the binding affinity of AVC to wild-type CCR5 ($CCR5_{WT}$) was the greatest with a K_D value of 2.9 nM as compared with SCH-C and TAK-779 with K_D values of 16.0 and 30.2 nM, respectively (Table 1). It was also noted that the number of mutations that affected the binding of AVC was greater than in the cases of TAK-779 and SCH-C (Table 1). Moreover, the amino acid substitutions with which AVC turned out to have different K_D values were mostly located in the second extracellular loop (ECL2) and its interface with TM4 (Gly^{163}), or TM5 (Lys^{191}). By contrast, with regard to SCH-C and TAK-779, no substantially different K_D values were obtained with amino acid substitutions in ECL2 (Table 1). The data suggest that not only the binding interactions but also the molecular size and/or bulkiness of AVC are related to the different numbers of K_D-affecting mutations and different profile of K_D values obtained and that AVC forms substantial hydrophobic contacts with and fits well inside the hydrophobic cavity within CCR5 (Fig. 4*A*). It was also thought that such tight interactions of AVC with residues in ECLs and the interface of extracellular and transmembrane domains of CCR5 are responsible for the greater binding affinity of AVC to CCR5 as compared with two other inhibitors.

It was intriguing that certain amino acids such as Gly^{163} and Lys^{191} formed critical hydrogen bond networks in the interaction of AVC and CCR5 (Fig. 3, *A* and *B*). It was thought, therefore, that the amino acid substitutions in such positions dramatically altered the binding affinity of AVC to CCR5. It is also noteworthy that Cys^{178} of ECL2 is presumed to form a putative disulfide bridge with Cys^{101} of ECL1 and to be critical for the conformation of CCR5 (34). In the present study, C178A substitution, which should disrupt the putative disulfide bridge and cause significant conformational changes in both ECL1 and ECL2, nullified the CCR5 binding affinity of AVC, but not of SCH-C or TAK-779 (Table 1). In this respect, the lesser interactions of SCH-C and TAK-779 with extracellular domains (Table 1) are likely responsible for the lack of influence of the C178A substitution on the binding affinity of SCH-C and TAK-779, corroborating the notion that mutations in ECL2 did not alter the binding of SCH-C and TAK-779 to CCR5 (Table 1).

Two events are likely involved in the reduced binding of inhibitors to CCR5 with an amino acid substitution(s): (i) the alteration of direct interaction, if present, between the amino acid residue and the inhibitor and/or (ii) an allosteric effect(s) in which there is a significant conformational change(s) of CCR5 either near or distant from the mutated residue. In this respect, in the present work, we have shown that multiple hydrogen bond networks are important for the binding of AVC to CCR5 (Fig. 3, *A* and *B*). Some residues such as Lys^{191} directly interact with AVC, and hence mutations that lose this direct interaction are very likely responsible for the loss of binding. The lack of drastic changes in the binding of SCH-C and TAK-779, which are not predicted to directly interact with Lys^{191}, also supports this inference. Gly^{163}, however, does not directly bind to AVC but is a critical part of the Gly^{163}-Ser^{180}-Lys^{191}-Thr^{195} hydrogen network (Fig. 3*A*). Our molecular modeling, however, indicates that arginine at position 163 does not form hydrogen bonds with Ser^{180} or Lys^{191}. This alteration in the hydrogen bond network probably changes the shape of the cavity in the ECL2-TM4-TM5 region (an allosteric effect near the mutated residue) and results in reduced binding of AVC to $CCR5_{G163R}$. Mutation at residue 283 might be an example of the one causing an allosteric conformational change(s) distant from the mutated residue. Only AVC is predicted to directly interact with Glu^{283}, but a E283A mutation results in significant loss of binding for all three inhibitors examined. Thus, it is thought that certain amino acid substitutions reduce the binding of an inhibitor even though they are not directly interacting with the inhibitor. It is also of note that mutations at certain residues directly interacting with an inhibitor do not always cause significant loss of binding if CCR5 does not undergo a conformational change(s) or takes an alternate conformation that is not unfavorable for inhibitor binding.

Because a crystal structure of CCR5 is not available, unlike other targets for intervention of HIV infection including HIV reverse transcriptase (36), in the present study, in an attempt to conduct structural analyses of the interactions of CCR5 inhibitors with various mutant CCR5 species, an initial structural model of CCR5 was generated using homology modeling based on the crystal structure of bovine rhodopsin (23). The present approach of combining the site-directed mutagenesis-based data (Table 1) and molecular modeling should be a valuable strategy for gaining structural insights for membrane-bound proteins for which x-ray crystal structures are not as yet available. The CCR5-inhibitor complex structures were defined by iterative optimization of CCR5 and inhibitor structures. Mutated CCR5 structures were also defined and optimized based on the wild-type CCR5 structure, and minimized structures of various CCR5 mutants were used as starting structures for obtaining docked complexes of mutated CCR5 with inhibitors. It is of note that in the present study, our modeling study was combined and fine-tuned with the results of the saturation binding assay using a panel of mutant CCR5-expressing cells and tritiated CCR5 inhibitors and the resultant configuration and orientation of inhibitors docked within the hydrophobic cavity of CCR5 yielded a consistent analysis of the structure-activity data. The conformations of CCR5 without an inhibitor and CCR5 bound to an inhibitor are likely to be substantially different from each other because conformational changes are expected to occur upon inhibitor binding to CCR5. Thus, the conformational flexibility of both inhibitors and CCR species were taken into account in our analysis. In this regard, our ongoing analyses of binding affinity profiles using different ^3H-labeled CCR5 inhibitors and an expanded panel of mutant CCR5-expressing cell lines should further illuminate the intramolecular and intermolecular interactions of CCR5 and CCR5 inhibitors.

We also examined the binding profile of CCR5 inhibitors when one inhibitor was added to CCR5-overexpressing cells, followed by the addition of the second inhibitor (Fig. 7). Interestingly, when AVC first bound to CCR5 and SCH-C or TAK-779 was subsequently added, both SCH-C and TAK-779 only partially displaced AVC (Fig. 7, *A* and *B*). However, when SCH-C or TAK-779 first bound to CCR5 and AVC was subsequently added, SCH-C and TAK-779 were substantially displaced by AVC (Fig. 7, *C* and *D*). This ineffective displacement of AVC once bound to $CCR5_{WT}$ by SCH-C and TAK-779 could be explained by the difference of their K_D values (2.9 nM for AVC, 16 nM for SCH-C, and 30.2 nM for TAK-779 as illustrated in Table 1). However, it is of note that both SCH-C and TAK-779 failed to displace AVC even with very high concentrations: 3,333-fold (10 μM; Fig. 7*A*) and 20,833-fold (62.5 μM; Fig. 7*B*), respectively, greater than the [^3H]AVC concentration (3 nM). Thus, only the difference in K_D values among the three inhibitors unlikely fully explains the failure of AVC replacement by SCH-C and TAK-779. In this regard, a possible explanation is that AVC induces a series of significant conformational changes in CCR5 and, upon the completion of its stable lodging within the hydrophobic cavity within $CCR5_{WT}$, the binding and/or entry into CCR5 of the second inhibitor is

hindered and the interaction between AVC and the second inhibitor added is no longer merely competitive. Although the data of displacement experiments using two CCR5 inhibitors discussed above may not offer a clear mechanistic explanation at present due to the limitation of the currently available methodologies, the data may have a clinical relevance in the future because more than one CCR5 inhibitor may be simultaneously administered when multiple CCR5 inhibitors are introduced in the therapy of AIDS. It is also noteworthy that the tight CCR5 binding profile of AVC is presumably related to the extensive and prolonged CCR5 occupancy observed in phytohemagglutinin-activated peripheral blood mononuclear cells ($t_{1/2} \sim 9$ h) (12) and in circulating lymphocytes in HIV-1-negative and HIV-1-positive individuals ($t_{1/2}$ of 69–152 h depending on different AVC doses), a potentially favorable feature that could enable once daily (*QD*) or twice daily (*BID*) administration of AVC.

In the present study, we observed that amino acid mutations within the transmembrane domains such as Y108A, G163R, and I198A exerted only minimal or moderate effects on the binding of CC-chemokines to CCR5 (Fig. 8*B*), whereas they caused a substantial reduction in HIV-1-gp120/CD4 complex binding to CCR5 (Fig. 8*A*) and a more drastic reduction in the susceptibility to HIV-1 infection (Fig. 8*C*). It is possible that the molecular size of the gp120/CD4 complex is far greater and its interactions with CCR5 are more extensive compared with the case of CC-chemokines, and therefore, the process for establishing HIV-1 infection is more extensively affected by such amino acid substitutions in comparison to CCR5 binding of CC-chemokines and the ensuing signal transduction. In this regard, a large body of literature has shown that CCR5 regions to which the envelope glycoproteins of HIV-1 bind are functionally and structurally quite different from those to which CC-chemokines bind (19–21, 32, 33). Wu *et al.* (20) and Lee *et al.* (21) demonstrated that a group of NH_2 terminus-specific CCR5 monoclonal antibodies did not block the binding of or Ca^{2+} flux induction by CC-chemokines, although ECL2-specific monoclonal antibodies effectively block the binding of CC-chemokines and their Ca^{2+} flux induction. Navenot *et al.* (33) subsequently confirmed these notions and further demonstrated that a CCR5 chimera with the NH_2 terminus of CXCR2 bound MIP-1α with an affinity similar to that of $CCR5_{WT}$. In contrast, both NH_2 terminus- and ECL2-specific mAbs reportedly blocked efficiently the binding of gp120 to CCR5 although the latter mAbs caused superior inhibition (20, 21). These previously published data strongly suggest that the interactions of CCR5 with HIV-1-glycoproteins involve multiple CCR5 domains and consist of more complex processes, whereas those with CC-chemokines involve fewer CCR5 domains and potentially fewer processes. Thus, this implies that the intervention of HIV-1 infection without interrupting physiological CC-chemokine/CCR5 interactions should be feasible. Indeed, AVC does not potently block the physiologic CC-chemokine/CCR5 interactions, although it highly efficiently suppresses the infection of HIV-1 with IC_{50} values of subnanomolar concentrations (11).

Taken together, mutations associated with AVC binding to CCR5 decreased gp120 binding to CCR5 and the susceptibility to HIV-1 infection, whereas mutations in TM4 and TM5 that also decreased gp120 binding and HIV-1 infectivity had less effects on the binding of CC-chemokines, suggesting that CCR5 inhibition targeting appropriate regions might render the inhibition highly HIV-1-specific, preserving the CC chemokine-CCR5 interactions. The present data should not only help design more potent and HIV-1-specific CCR5 inhibitors, but also should give new insights into the dynamics of CC-chemokine-CCR5 interactions and the mechanisms of CCR5 involvement in the process of cellular entry of HIV-1.

Acknowledgments—We thank Steve LaFon, James Demarest, Alphonso Nillas, Larry Boone, Yashuhiro Koh, Yosuke Maeda, and Philip Yin for helpful discussion and/or critical reading of the manuscript. We also thank the Center for Information Technology, National Institutes of Health, for providing computational resources.

REFERENCES

1. Fauci, A. S. (2003) *Nat. Med.* **9**, 839–843
2. Mitsuya, H., and Erickson, J. (1999) in *Textbook of AIDS Medicine* (Merigan, T. C., Bartlet, J. G., and Bolognesi, D., eds) pp. 751–780, Williams and Wilkins, Baltimore
3. Siliciano, J. D., Kajdas, J., Finzi, D., Quinn, T. C., Chadwick, K., Margolick, J. B., Kovacs, C., Gange, S. J., and Siliciano, R. F. (2003) *Nat. Med.* **9**, 727–728
4. Richman, D. D. (2001) *Nature* **410**, 995–1001
5. Department of Health and Human Services (DHHS) (2005) *Guidelines for the Use of Antiretroviral Agents in HIV-1-infected Adults and Adolescents*
6. Raport, C. J., Gosling, J., Schweickart, V. L., Gray, P. W., and Charo, I. F. (1996) *J. Biol. Chem.* **271**, 17161–17166
7. Alkhatib, G., Combadiere, C., Broder, C. C., Feng, Y., Kennedy, P. E., Murphy, P. M., and Berger, E. A. (1996) *Science* **272**, 1955–1958
8. Deng, H., Liu, R., Ellmeier, W., Choe, S., Unutmaz, D., Burkhart, M., Di Marzio, P., Marmon, S., Sutton, R. E., Hill, C. M., Davis, C. B., Peiper, S. C., Schall, T. J., Littman, D. R., and Landau, N. R. (1996) *Nature* **381**, 661–666
9. Trkola, A., Dragic, T., Arthos, J., Binley, J. M., Olson, W. C., Allaway, G. P., Cheng-Mayer, C., Robinson, J., Maddon, P. J., and Moore, J. P. (1996) *Nature* **384**, 184–187
10. Wu, L., Gerard, N. P., Wyatt, R., Choe, H., Parolin, C., Ruffing, N., Borsetti, A., Cardoso, A. A., Desjardin, E., Newman, W., Gerard, C., and Sodroski, J. (1996) *Nature* **384**, 179–183
11. Maeda, K., Nakata, H., Koh, Y., Miyakawa, T., Ogata, H., Takaoka, Y., Shibayama, S., Sagawa, K., Fukushima, D., Moravek, J., Koyanagi, Y., and Mitsuya, H. (2004) *J. Virol.* **78**, 8654–8662
12. Nakata, H., Maeda, K., Miyakawa, T., Shibayama, S., Matsuo, M., Takaoka, Y., Ito, M., Koyanagi, Y., and Mitsuya, H. (2005) *J. Virol.* **79**, 2087–2096
13. Baba, M., Nishimura, O., Kanzaki, N., Okamoto, M., Sawada, H., Iizawa, Y., Shiraishi, M., Aramaki, Y., Okonogi, K., Ogawa, Y., Meguro, K., and Fujino, M. (1999) *Proc. Natl. Acad. Sci. U. S. A.* **96**, 5698–5703
14. Strizki, J. M., Xu, S., Wagner, N. E., Wojcik, L., Liu, J., Hou, Y., Endres, M., Palani, A., Shapiro, S., Clader, J. W., Greenlee, W. J., Tagat, J. R., McCombie, S., Cox, K., Fawzi, A. B., Chou, C. C., Pugliese-Sivo, C., Davies, L., Moreno, M. E., Ho, D. D., Trkola, A., Stoddart, C. A., Moore, J. P., Reyes, G. R., and Baroudy, B. M. (2001) *Proc. Natl. Acad. Sci. U. S. A.* **98**, 12718–12723
15. Gribble, G. W. (1975) *J. Chem. Soc. Chem. Commun.* 535–541
16. Evans, E. A. (1974) in *Tritium and Its Compounds* (Evans, E. A., ed) pp. 271–317, J. Wiley and Sons, New York
17. Maeda, K., Yoshimura, K., Shibayama, S., Habashita, H., Tada, H., Sagawa, K., Miyakawa, T., Aoki, M., Fukushima, D., and Mitsuya, H. (2001) *J. Biol. Chem.* **276**, 35194–35200
18. Maeda, Y., Foda, M., Matsushita, S., and Harada, S. (2000) *J. Virol.* **74**, 1787–1793
19. Siciliano, S. J., Kuhmann, S. E., Weng, Y., Madani, N., Springer, M. S., Lineberger, J. E., Danzeisen, R., Miller, M. D., Kavanaugh, M. P., DeMartino, J. A., and Kabat, D. (1999) *J. Biol. Chem.* **274**, 1905–1913
20. Wu, L., LaRosa, G., Kassam, N., Gordon, C. J., Heath, H., Ruffing, N., Chen, H., Humblias, J., Samson, M., Parmentier, M., Moore, J. P., and Mackay, C. R. (1997) *J. Exp. Med.* **186**, 1373–1381
21. Lee, B., Sharron, M., Blanpain, C., Doranz, B. J., Vakili, J., Setoh, P., Berg, E., Liu, G., Guy, H. R., Durell, S. R., Parmentier, M., Chang, C. N., Price, K., Tsang, M., and Doms, R. W. (1999) *J. Biol. Chem.* **274**, 9617–9626
22. Maeda, Y., Venzon, D. J., and Mitsuya, H. (1998) *J. Infect. Dis.* **177**, 1207–1213
23. Palczewski, K., Kumasaka, T., Hori, T., Behnke, C. A., Motoshima, H., Fox, B. A., Le Trong, I., Teller, D. C., Okada, T., Stenkamp, R. E., Yamamoto, M., and Miyano, M. (2000) *Science* **289**, 739–745
24. Halgren, T. A., Murphy, R. B., Friesner, R. A., Beard, H. S., Frye, L. L., Pollard, W. T., and Banks, J. L. (2004) *J. Med. Chem.* **47**, 1750–1759
25. Xiang, Z., and Honig, B. (2001) *J. Mol. Biol.* **311**, 421–430
26. Kaminski, G. A., Friesner, R. A., Tirado-Rives, J., and Jorgensen, W. J. (2001) *J. Phys. Chem. B* **105**, 6474–6487
27. Friesner, R. A., Banks, J. L., Murphy, R. B., Halgren, T. A., Klicic, J. J., Mainz, D. T., Repasky, M. P., Knoll, E. H., Shelley, M., Perry, J. K., Shaw, D. E., Francis, P., and Shenkin, P. S. (2004) *J. Med. Chem.* **47**, 1739–1749
28. Exner, T. E., Keil, M., Moeckel, G., and Brickmann, J. (1998) *J. Mol. Model* **4**, 340–343
29. Viswanadhan, V. N., Ghose, A. K., Revankar, G. R., and Robins, R. K. (1989) *J. Chem. Inf. Comput. Sci.* **29**, 163–172

30. Dragic, T., Trkola, A., Thompson, D. A., Cormier, E. G., Kajumo, F. A., Maxwell, E., Lin, S. W., Ying, W., Smith, S. O., Sakmar, T. P., and Moore, J. P. (2000) *Proc. Natl. Acad. Sci. U. S. A.* **97,** 5639–5644
31. Tsamis, F., Gavrilov, S., Kajumo, F., Seibert, C., Kuhmann, S., Ketas, T., Trkola, A., Palani, A., Clader, J. W., Tagat, J. R., McCombie, S., Baroudy, B., Moore, J. P., Sakmar, T. P., and Dragic, T. (2003) *J. Virol.* **77,** 5201–5208
32. Dragic, T., Trkola, A., Lin, S. W., Nagashima, K. A., Kajumo, F., Zhao, L., Olson, W. C., Wu, L., Mackay, C. R., Allaway, G. P., Sakmar, T. P., Moore, J. P., and Maddon, P. J. (1998) *J. Virol.* **72,** 279–285
33. Navenot, J. M., Wang, Z. X., Trent, J. O., Murray, J. L., Hu, Q. X., DeLeeuw, L., Moore, P. S., Chang, Y., and Peiper, S. C. (2001) *J. Mol. Biol.* **313,** 1181–1193
34. Blanpain, C., Lee, B., Vakili, J., Doranz, B. J., Govaerts, C., Migeotte, I., Sharron, M., Dupriez, V., Vassart, G., Doms, R. W., and Parmentier, M. (1999) *J. Biol. Chem.* **274,** 18902–18908
35. Govaerts, C., Bondue, A., Springael, J. Y., Olivella, M., Deupi, X., Le Poul, E., Wodak, S. J., Parmentier, M., Pardo, L., and Blanpain, C. (2003) *J. Biol. Chem.* **278,** 1892–1903
36. Sarafianos, S. G., Das, K., Hughes, S. H., and Arnold, E. (2004) *Curr. Opin. Struct. Biol.* **14,** 716–730
37. Sparks, S., Adkison, K., Shachoy-Clark, A., Piscitelli, S., and Demarest, J. (2005) *12th Conference on Retroviruses and Opportunistic Infections, Boston, February 22–25, 2005,* Abstr. 77, Foundation for Retrovirology and Human Health, Alexandria, VA
38. Lalezari, J., Thompson, M., Kumar, P., Piliero, P., Davey, R., Murtaugh, T., Patterson, K., Shachoy-Clark, A., Adkinson, A., Demarest, J., Sparks, S., Fang, L., Lou, Y., Berrey, M., and Piscitelli, S. (2004) *44th Interscience Conference on Antimicrobial Agents and Chemotherapy, Boston, February 22–25, 2005,* Abstr. H-1137b, Foundation for Retrovirology and Human Health, Alexandria, VA

Resistance profile of a neutralizing anti-HIV monoclonal antibody, KD-247, that shows favourable synergism with anti-CCR5 inhibitors

Kazuhisa Yoshimura[a], Junji Shibata[a], Tetsuya Kimura[a], Akiko Honda[a], Yosuke Maeda[b], Atsushi Koito[a], Toshio Murakami[c], Hiroaki Mitsuya[d] and Shuzo Matsushita[a]

Background: The high-affinity humanized monoclonal antibody (MAb) KD-247 reacts with a tip region in gp120-V3 and cross-neutralizes primary isolates with a matching neutralization sequence motif.

Methods: We induced an HIV-1 variant that was resistant to KD-247 by exposing the JR-FL virus to increasing concentrations of KD-247 in PM1/CCR5 cells, which expressed high levels of CCR5 *in vitro*. We determined the amino acid sequence of the gp120-encoding region of the JR-FL escape mutant from KD-247. To confirm that this substitution was responsible for the KD-247-resistance, a single-round replication assay was performed. We further evaluated the anti-HIV-1 interactions between KD-247 and various CCR5 inhibitors *in vitro*.

Results: At passage 8 of the culture in the presence of 1000 μg/ml KD-247, one amino acid substitution, Gly to Glu at position 314 (G314E), was identified in the V3-tip of gp120. A pseudotyped virus with the G314E mutation was highly resistant to KD-247. Unexpectedly, this mutant virus was sensitive to CCR5 inhibitors, RANTES, recombinant human soluble CD4 (rsCD4) and an anti-CCR5 MAb, but resistant to an anti-CD4 MAb, compared with the wild-type virus. We also found that combinations of KD-247 and CCR5 inhibitors were highly synergistic.

Conclusions: The present data suggest that KD-247 has certain advantages for possible passive immunotherapy. They are: high concentrations of KD-247 are needed for viral acquisition of KD-247 resistance; the escape variants are more sensitive to CCR5 inhibitors and rsCD4; and there are high levels of synergism between KD-247 and CCR5 inhibitors at all concentrations tested.

AIDS 2006, **20**:2065–2073

Keywords: HIV-1, KD-247, anti-V3 monoclonal antibody, broadly neutralizing, CCR5 inhibitor, synergism

From the [a]Division of Clinical Retrovirology and Infectious Diseases, Center for AIDS Research, Graduate School of Medical Sciences, Kumamoto University, Kumamoto, Japan, the [b]Department of Medical Virology, Graduate School of Medical Sciences, Kumamoto University, Kumamoto, Japan, the [c]The Chemo-Sero-Therapeutic Research Institute, Kyokushi, Kikuchi, Kumamoto, Japan, and the [d]Department of Internal Medicine II, Graduate School of Medical Sciences, Kumamoto University, Kumamoto, Japan.

Correspondence to S. Matsushita, Division of Clinical Retrovirology and Infectious Diseases, Center for AIDS Research, Kumamoto University, Kumamoto 860-0811, Japan.

Tel: +81 96 373 6536; fax: +81 96 373 6537; e-mail: shuzo@kaiju.medic.kumamoto-u.ac.jp

These data were presented at the *Thirteenth Conference on Retroviruses and Opportunistic Infections*. Denver, CO, February 2006 [abstract 506].

Note: K. Yoshimura and J. Shibata contributed equally to this work.

Received: 21 February 2006; accepted: 27 July 2006.

Introduction

In a recent paper, we described a cross-neutralizing anti-V3 antibody, KD-247, against primary isolates via sequential immunization with six peptides from V3 that contained a neutralizing epitope of HIV-1 [1]. The ability of KD-247 to neutralize HIV-1 may be dependent on site-specific binding to an epitope on the viral envelope glycoprotein. The complementarity determining regions of KD-247 were transferred from the mouse monoclonal antibody (MAb) C25, which was designed to have broad neutralization activity against HIV-1 clade B isolates. The recognition site of KD-247 was mapped to five or six amino acids around the PGR core sequence at the tip of the V3 region of gp120. The shortest reactive peptide recognized by KD-247 was determined to be IGPGR, although the epitope was stabilized by the addition of one or more supplemental amino acids. The GPGR sequence in the V3 tip is highly conserved among HIV-1 strains [2]. In a recent study, we showed that the reshaped MAb KD-247 was suitable for use not only as an antibody for passive immunization for the prevention of HIV infection but also as an antibody for passive transfer immunotherapy for infected individuals [3].

In the present study, we induced HIV-1 variants that escaped from neutralization by KD-247 *in vitro* by continuously exposing the R5 virus JR-FL to increasing concentrations of KD-247 and defined the virological properties of a pseudotyped HIV-1 clone carrying the KD-247 escape-associated *env* gene mutation. We also evaluated the anti-HIV-1 interactions between KD-247 and various CCR5 inhibitors *in vitro*.

Materials and methods

Cells, culture conditions and reagents

The CD4-positive T-cell line PM1 was maintained in RPMI 1640 (Sigma, St. Louis, Missouri, USA) supplemented with 10% heat-inactivated foetal calf serum (Hyclone, Logan Utah, USA), 50 U/ml penicillin and 50 μg/ml streptomycin. PM1/CCR5 cells were generated by standard retrovirus-mediated transduction of PM1 cells with pBABE-CCR5 provided by the National Institutes of Health AIDS Research and Preference Reagent Program [4]. PM1 and PM1/CCR5 cells were analysed for their surface expressions of CD4, CCR5 and CXCR4 using a FACSCalibur (Becton Dickinson, Franklin Lakes, New Jersey, USA). 293T cells were maintained in Dulbecco's modified Eagle medium (DMEM; Sigma) supplemented with 10% heat-inactivated FCS. The CD4 human osteogenic sarcoma cell line GHOST was maintained in DMEM supplemented with 10% FCS, 200 μg/ml G418 (Gibco BRL, Rockville, Maryland, USA) and 100 μg/ml hygromycin B (Sigma). The GHOST derivatives GHOST-hi5 and GHOST-CXCR4 stably expressed CCR5 and CXCR4, respectively, as described elsewhere [5], and were selected with 1 μg/ml puromycin (Sigma).

17b, a CD4-induced (CD4i) MAb, was a kind gift from J. Robinson (Department of Pediatrics, Tulane University Medical Center, New Orleans, Louisiana, USA). 447-52D, an anti-gp120 V3 MAb, was a kind gift from S. Zolla-Pazner (Department of Pathology, New York University School of Medicine, New York, USA). 2D7, an anti-CCR5 MAb, and RPA-T4, an anti-CD4 MAb, were purchased from BD Biosciences Pharmingen (San Jose, California, USA). 2′,3′-dideoxyinosine (ddI, didanosine) was from Calbiochem, San Diego, California, USA. 3′-thiacytidine (3TC, lamivudine) was a kind gift from R. F. Schinazi (Department of Pediatrics, Emory University School of Medicine, Atlanta, Georgia, USA). Saquinavir (SQV) was kindly provided by Roche Products Ltd., Welwyn Garden City, UK. Amprenavir (APV) was a kind gift from GlaxoSmithKline, Middlesex, UK. Nelfinavir (NFV) and indinavir (IDV) were kindly provided by Japan Energy Inc., Tokyo, Japan. Recombinant human soluble CD4 (rsCD4), MIP-1α, MIP-1β and RANTES were from R&D Systems Inc., Abingdon, UK. The CCR5 inhibitors TAK-779 [6] and SCH-351125 (SCH-C) [7] were synthesized as previously described. AK-602, a CCR5 inhibitor, was kindly provided by Ono Pharmaceutical Co. Ltd., Osaka, Japan [8].

Isolation of a KD-247-resistant mutant from JR-FL *in vitro*

For the selection of a KD-247 escape virus, JR-FL [9] was treated with various concentrations of KD-247 and then infected into PM1/CCR5 cells as previously described with minor modifications [10]. Viral replication was monitored by observation of any cytopathic effects in PM1/CCR5 cells. The culture supernatant was harvested on day 7 and used to infect fresh PM1/CCR5 cells for the next round of culture in the presence of increasing concentrations of KD-247. After the virus was passaged in the presence of up to 1000 μg/ml KD-247 in PM1/CCR5 cells, a KD-247-resistant virus, JR-FL(1000)8P, was recovered from the cell culture supernatant. JR-FL was also passaged for the same time periods in PM1/CCR5 cells in the absence of KD-247 to exclude any effects of the long-term culture of eight passages, and the resulting virus was designated JR-FL(−)8P.

The sensitivities of the passage 8 JR-FL viruses in the presence or absence of KD-247 to various drugs or MAb were determined as previously described with minor modifications [11]. Briefly, PM1-CCR5 cells (2×10^3/well) were exposed to 100 50% tissue culture inhibitory doses ($TCID_{50}$) of the JR-FL(1000)P8 or JR-FL(−)P8 in the presence of various concentrations of drugs or MAb in 96-well round-bottom plates. The 50% inhibitory concentration (IC_{50}) values were determined using the MTT {3-(4,5-Dimethylthiazol-2-yl)-2,5-diphenyltetrazolium

bromide} (MTT) assay on day 7 of culture. All assays were performed in duplicate.

Viral RNA (0.5 μg) extracts from cell culture supernatants at several concentrations of KD-247 were reverse-transcribed using a High Capacity cDNA Archive Kit (Applied Biosystems, Foster City, California, USA). The cDNA obtained were subjected to PCR amplification using *Taq* polymerase. After cloning the amplified products into pCR2.1, the Env regions in both the passaged and selected viruses were sequenced using an ABI PRISM 310 automated DNA sequencer (Applied Biosystems).

Construction of mutant envelope expression vectors and production of pseudovirions

For the construction of mutant envelope expression vectors, we used pCXN2, which contains a chicken actin promoter. Briefly, the JR-FL *env* region was cloned by PCR and ligated into pCR2.1, generating pCR2-FL_{wt}. The *Eco*RI fragment of pCR2-FL_{wt} containing the entire *env* region was ligated into pCXN2 to give pCXN-FL_{wt} [9]. A mutant Env (G314E) expression vector was generated from pCXN-FL_{wt} using a QuikChange site-directed mutagenesis kit (Stratagene, Chedar Creek, Texas, USA) and the primers JR-FLv3G/Efw (5′–TACATA-TAGGACCAGAGAGAGCATTTTATAC–3′) and JR-FLv3G/Erv (5′–GTATAAAATGCTCTCTCTGGTCC TATATGTA–3′) according to the manufacturer's protocol, and designated pCXN-FLG314E.

Plasmids pNL4-3.Luc.R^-E^- and pRSV-Rev [12], supplied by the NIH AIDS Research and Reference Reagent Program, and plasmid pCXN2, expressing wild-type or G314E Env, were cotransfected into 293T cells using the Effectene Transfection Reagent (Qiagen, Valencia, California, USA). At 24 h after the transfection, the pseudovirus-containing supernatants were harvested, filtered through a 0.2-μm pore-size filter and stored at −150°C. For measurement of the pseudovirus activities, a luminescence assay with GHOST-hi5 cells was used as previously described [13].

Neutralization assays

A single-cycle infectivity assay was used to measure the neutralization of JR-FL_{wt} or JR-FL_{GPER} pseudovirions as described previously [13]. Briefly, MAb at various concentrations and a pseudovirus suspension corresponding to 200 $TCID_{50}$ were preincubated for 15 min on ice. The virus–antibody mixtures were added to GHOST-hi5 cells, which had been seeded in a 96-well plate (1.5×10^4 cells/well) on the previous day. The cultures were incubated for 2 days at 37°C, washed with phosphate-buffered saline and lysed with lysis buffer (Luc PGC-50; PicaGene, Tokyo, Japan). Following transfer of the cell lysates to luminometer plates (Costar 3912), the luciferase activity (in relative light units) in each well was measured using Luciferase Substrate (100 μl/well; PicaGene) in a TR717 microplate luminometer (Applied Biosystems). The reduction in infectivity was determined by comparing the relative light units in the presence and absence of MAb and expressed as the percent neutralization. The same assay was repeated two to three times.

In vitro binding assay to the JR-FL_{wt} or JR-FL_{GPER} envelope

The JR-FL gp160 coding sequence was amplified from the infectious clone vector (pJR-FL) using the primers ENVA-*Eco*RI (5′–CGGAATTCGGCTTAGGCATCT CCTATGGCAGGAAGAA–3′) and ENVN-*Bam*HI (5′–CGGGATCCCGCTGCCAATCAGGGAAGTAG CCTTGTGT–3′). The product was digested with *Eco*RI and *Bam*HI and subcloned into the corresponding sites in pDNR-1r (Clontech) for sequencing and subsequent manipulation. A JR-FL_{GPER} Env expression vector was generated from pDNR-JR-FL_{wt} using a QuikChange site-directed mutagenesis kit and the primers JR-FLv3G/Efw and JR-FLv3G/Erv according to the manufacturer's protocol. The wild-type and mutated *env* gene fragments were then subcloned into pLP-IRES2-EGFP (Clontech) using Cre-recombinase (Clontech) according to the manufacturer's instructions, and designated pLP-EGFP-JR-FL_{wt} and pLP-EGFP-JR-FL_{GPER}, respectively.

293T cells were cotransfected with pRSV-Rev (0.5 μg) and pLP-IRES2-EGFP, pLP-EGFP-JR-FL_{wt} or pLP-EGFP-JR-FL_{GPER} (9.5 μg) using the Effectene Transfection Reagent (Qiagen). After 36 h, the cells were harvested, incubated with each anti-HIV-1 MAb with or without rsCD4 (0.5 μg/ml) in combination with biotin-conjugated anti-human IgG and peridinin chlorophyll-a protein-conjugated streptavidin (BD Biosciences Pharmingen), gated for the GFP-positive area and analysed using a FACSCalibur.

Data analysis and evaluation of synergy

Analysis of the synergistic, additive or antagonist effects of the antiviral agents was first performed according to the median effect principle using the CalcuSyn version 2 computer program [14,15] to provide estimates of the IC_{50} values of the antiviral reagents in different combinations. Combination indices (CI) were estimated from the data and reflected the nature of the interactions between KD-247 and the CCR5 inhibitors against JR-FL(−)8P in PM1/CCR5 cells, as evaluated using the MTT assay. Specifically, $CI < 0.9$ indicated synergy, $0.9 < CI < 1.1$ indicated additivity and $CI > 1.1$ indicated antagonism. The value of CI was directly proportional to the amount of synergy in the combination regimen. For example, values of $CI < 0.5$ represented a high degree of synergy, whereas values of $CI > 1.5$ represented significant antagonism. This approach has been widely used in analyses of antiviral interactions and was chosen to allow comparability with published literature.

Statistical analysis

Statistical correlations were analysed using Student's t test. P values < 0.05 were considered statistically significant.

Results

Selection of a KD-247 escape variant

For the isolation of a KD-247 escape mutant from R5 HIV *in vitro*, PM1 cells expressing high levels of CCR5, designated PM1/CCR5 cells, which were highly sensitive to both X4 and R5 HIV infection and accompanied by prominent syncytia [4] were used as the target cells. An R5 HIV strain, JR-FL, which uses CCR5 as its coreceptor was used for the selection of a KD-247 escape virus.

In order to select an HIV-1 variant that can escape from neutralization by KD-247 *in vitro*, we exposed PM1/CCR5 cells to JR-FL, and serially passaged the virus in the presence of increasing concentrations of KD-247, or in the absence of the MAb as a control. The selected virus was initially propagated in the presence of 1 μg/ml KD-247, and during the course of the selection procedure, the MAb concentration was increased to 1000 μg/ml. At passage 8, the supernatants containing the passaged viruses in the presence or absence of KD-247, designated JR-FL(1000)8P and JR-FL(−)8P, respectively, were harvested and titrated for their infectivities and sensitivities to KD-247, CCR5 inhibitors (TAK-779, SCH-C and AK-602), nucleoside reverse transcriptase inhibitors (NRTI; ddI and 3TC) and protease inhibitors (PI; NFV, IDV, APV and SQV), as evaluated by the MTT assay (Table 1). The IC_{50} values of KD-247 against JR-FL(−)8P and JR-FL(1000)8P were 6.3 and > 100 μg/ml, respectively. The fold difference between these IC_{50} values was > 16. JR-FL(1000)8P was sensitive to all the NRTI and PI, similar to JR-FL(−)8P. Unexpectedly, JR-FL(1000)8P was more sensitive to the three CCR5 inhibitors (TAK-779, SCH-C and AK-602), rsCD4, anti-CCR5 MAb 2D7 and RANTES than JR-FL(−)8P. However, JR-FL(1000)8P was threefold more resistant to anti-CD4 MAb RPA-T4 than JR-FL(−)8P. These data suggest that the escape variant with a highly resistant phenotype against KD-247 becomes more sensitive to CCR5 inhibitors and rsCD4, and needs higher concentration of anti-CD4 antibody for entry blocking, compared with JR-FL(−)8P.

Sequencing of the envelope region of the KD-247 escape mutant

To determine the region responsible for the reduced sensitivity of the escape mutant to KD-247, the C1–C4 regions of the envelope were sequenced after cloning of the PCR product of each region using cDNA synthesized from viral RNA obtained from the supernatants of infected cells as templates. A total of 12–16 clones for each PCR product were isolated and sequenced. Analyses of the *env* sequences of these products revealed that the selected virus had a Gly→Glu substitution at codon 314 (G314E) in the V3 region of the envelope at passage 7 (600 μg/ml; 10/12 clones) and passage 8 (1000 μg/ml; 12/16 clones) (Fig. 1). Some changes in the envelope sequence in other regions, including C1, V1, V2, C2, C3, V4 and C4 of the escape mutant were found as well as in V3 around the IGPGR sequence even at early time points in the presence of the selective pressure. It is possible that these mutations also confer resistance to KD-247 but lead to virus of decreased fitness and thus they did not expand in a next passage except for the G314E. On the other hand, the virus passaged in PM1/CCR5 cells

Table 1. Anti-HIV-1 activities of various MAb and inhibitors toward KD247-resistant JR-FL.

Antibody or inhibitor	$IC_{50} \pm SD$[a]		Fold change	P[b]
	JR-FL(−)8P	JR-FL(1000)8P		
KD-247 (μg/ml)	6.3 ± 5.0	>100	<16	**<0.01**
TAK-779 (nM)	217 ± 50.3	54.7 ± 29.5	0.3	**<0.01**
SCH-C (nM)	27.5 ± 3.5	8.0 ± 1.4	0.3	**0.02**
AK-602 (nM)	7.1 ± 4.5	0.15 ± 0.08	0.02	**0.02**
Didanosine (μM)	1.0 ± 0.57	1.0 ± 0.27	1.0	0.98
Lamivudine (μM)	0.33 ± 0.01	0.29 ± 0.04	0.9	0.30
Nelfinavir (μM)	0.033 ± 0.001	0.036 ± 0.006	1.1	0.56
Indinavir (μM)	0.017 ± 0.004	0.016 ± 0.005	0.9	0.85
Amprenavir (μM)	0.022 ± 0.001	0.017 ± 0.008	0.8	0.47
Saquinavir (μM)	0.0038 ± 0.0004	0.0034 ± 0.0004	0.9	0.42
rsCD4 (μg/ml)	3.3 ± 0.07	0.57 ± 0.48	0.2	**0.02**
Anti-CD4 MAb (RPA-T4) (μg/ml)	0.01 ± 0.004	0.03 ± 0.004	3.0	**0.01**
Anti-CCR5 MAb (2D7) (μg/ml)	0.19 ± 0.03	0.066 ± 0.005	0.3	**0.03**
MIP-1α (μg/ml)	0.006 ± 0.002	0.0029 ± 0.001	0.5	0.11
MIP-1β (μg/ml)	0.39 ± 0.08	0.23 ± 0.18	0.6	0.22
RANTES (μg/ml)	0.045 ± 0.0007	0.005 ± 0.001	0.1	**0.02**

[a]PM1/CCR5 cells (2×10^3) were exposed to 100 TCID50 of JR-FL(−)8P or JR-FL(1000)8P and then cultured in the presence of various concentrations of MAb or inhibitors. The IC_{50} values were determined using the MTT assay on day 7 of culture. Data shown represent values derived from the results of two or three independent experiments conducted in duplicate.
[b]P values < 0.05 were considered statistically significant (shown in bold type). IC, Inhibitory concentration.

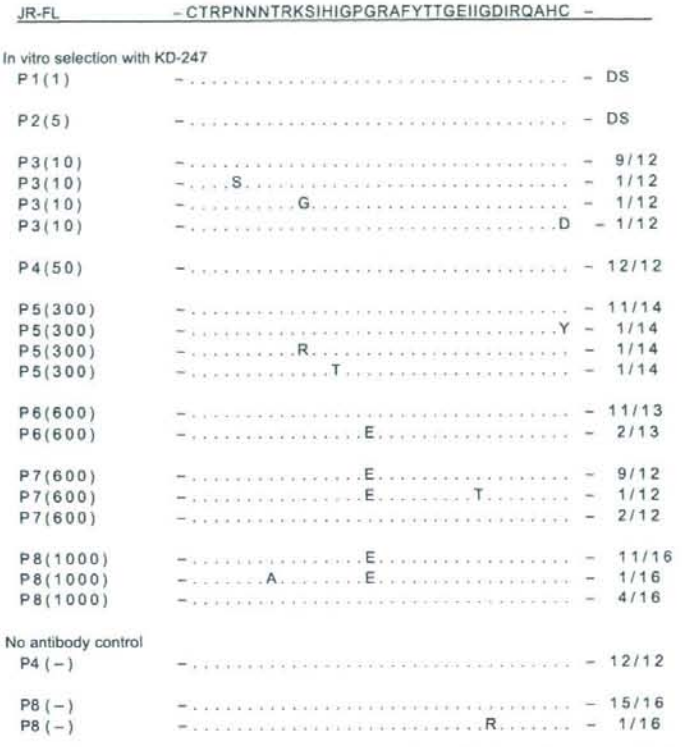

Fig. 1. V3 amino acid sequences from the supernatants of JR-FL-infected PM1/CCR5 cells passaged in the presence or absence of KD-247. Viral RNA from the cell culture supernatants at several concentrations of KD-247 was reverse-transcribed. After subjecting the obtained cDNA to PCR amplification and cloning, the *env* regions in the viruses passaged in the presence or absence of KD-247 were sequenced. The wild-type JR-FL amino acid sequence of V3 is shown at the top. The numbers on the right show the numbers of clones with the listed sequence among the total number of clones tested. In each set of clones, the deduced amino acid sequence of the V3 region was aligned by the single amino acid code. Dots denote sequence identity. DS, Direct sequence.

without KD-247 did not show the G314E substitution at either passage 4 (0/12 clones) or passage 8 (0/16 clones) (Fig. 1).

Susceptibilities of HIV-1 containing the KD-247-associated G314E substitution to MAb and drugs

To confirm whether the G314E mutation was responsible for the reduced sensitivity to KD-247, a single-round replication assay was performed. Luciferase-reporter viruses were pseudotyped with wild-type JR-FL (JR-FL_{wt}) or singly mutated with G314E (JR-FL_{G314E}) in the V3 region. As shown in Fig. 2a, JR-FL_{G314E} was completely resistant to KD-247 up to 100 μg/ml. We also examined the sensitivities of the pseudotyped clones to rsCD4, anti-CD4 MAb RPA-T4 and anti-CCR5 MAb 2D7 by a single-round replication assay (Fig. 2b–d). As expected, JR-FL_{G314E} was more sensitive to rsCD4 and 2D7, but fourfold more resistant to RPA-T4, compared to JR-FLwt, similar to the results for the passaged viruses with or without KD-247.

Next, we determined the sensitivities of JR-FL_{G314E} to three CCR5 inhibitors (TAK-779, SCH-C and AK-602). The IC_{50} values of TAK-779, SCH-C and AK-602 against JR-FL_{G314E} were 20-, 10- and 5-fold lower than the corresponding values against JR-FL_{wt}, respectively (Fig. 2e–g). These results confirmed that the G314E mutation was associated with the observed reduction in the sensitivities of JR-FL(1000)8P to KD-247 and RPA-T4, and also with the increased sensitivities to rsCD4, 2D7 and CCR5 inhibitors.

Next, we analysed the sensitivities of JR-FL_{wt} and JR-FL_{G314E} to another broad-specificity neutralizing anti-V3 MAb 447-52D and the CD4i MAb 17b (Fig. 2h and i). Interestingly, JR-FL_{G314E} was more sensitive to both 17b ($<$ 0.8-fold change in the IC_{50}) and 447-52D (0.1-fold change in the IC_{50}) than JR-FLwt (Fig. 2h and i). A similar result regarding neutralization sensitivity to 17b was reported when viruses were pretreated with rsCD4 [16]. In our result, JR-FL_{G314E} was more sensitive to 17b

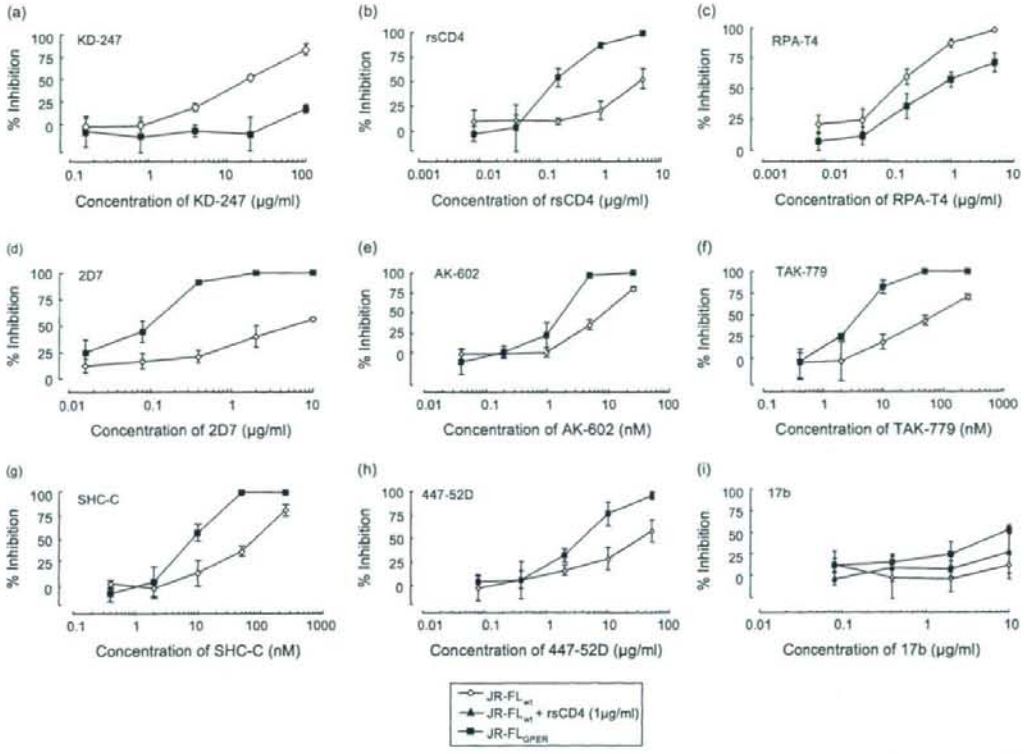

Fig. 2. Sensitivities of luciferase reporter HIV strains pseudotyped with the G314E envelope mutation to MAb, rsCD4 and CCR5 inhibitors. KD-247 (a), rsCD4 (b), 447-52D (h) and 17b with or without rsCD4 (1 μg/ml) (i) were preincubated with luciferase reporter HIVs pseudotyped with wild-type JR-FL (JR-FL$_{wt}$) or the G314E envelope mutant (JR-FL$_{GPER}$) for 15 min, followed by addition of the mixtures to the target cells (GOHST-hi5). The target cells were treated with RPA-T4 (c), 2D7 (d), AK-602 (e), TAK-779 (f) and SCH-C (g) for 15 min, followed by an inoculation of the pseudotype clones. Inhibitory effects were determined by measuring the luciferase activities on day 2 of culture.

than JR-FLwt preincubated with rsCD4 (1 μg/ml) (Fig. 2i).

Comparison of antibody binding to cell surface-expressed wild-type and GPER mutant Env

To elucidate the mechanism of the increased sensitivities of the escape virus with the G314E mutation in the V3-tip to 17b and 447-52D, wild-type or mutant Env-expressing 293T cells were established by transfecting each Env expression plasmid, and then stained with the MAb in the presence or absence of rsCD4 (0.5 μg/ml). Binding of a patient's IgG, KD-247, 17b or 447-52D to the surface-expressed Env proteins was assayed using a fluorescence-activated cell sorter analysis. As shown in Fig. 3, KD-247 bound to the wild-type JR-FL Env, but not the GPER mutant Env, while the other anti-V3 MAb, 447-52D, bound to both the Env proteins very well, especially the mutant Env. The mean fluorescence intensity (MFI) of 447-52D increased from 87.56 (wild-type Env) to 219.47 (GPER Env). Without rsCD4, the CD4i 17b MAb bound slightly to the wild-type Env (MFI, 33.21; Fig. 3) but failed to neutralize JR-FL$_{wt}$ (Fig. 2i). On the other hand, in the presence of rsCD4 (0.5 μg/ml), a shift in the MFI was observed with 17b binding to the surface of wild type-Env-expressing cells. In contrast to these data for wild-type Env, 17b bound to the mutant Env efficiently in the absence of rsCD4 at a higher level than to the wild-type Env in the presence of rsCD4 (MFI, 97.33 for the mutant Env versus 56.61 for the wild-type Env; Fig. 3). 17b was also able to neutralize JR-FL$_{GPER}$, even in the absence of rsCD4 (Fig. 2i). These results suggest that the G314E mutation in the V3-tip induces the expression of cryptic epitopes for antibodies against the CD4i epitope and V3 loop, such that the mutant virus is neutralized by the CD4i MAb without rsCD4 or by lower concentrations of the anti-V3 MAb compared with the wild-type virus.

Highly synergistic interactions of KD-247 combined with CCR5 inhibitors

Both neutralizing MAb and chemokine receptor inhibitors attack the viral entry process, especially at the stage of the chemokine receptor-gp120 (V3)

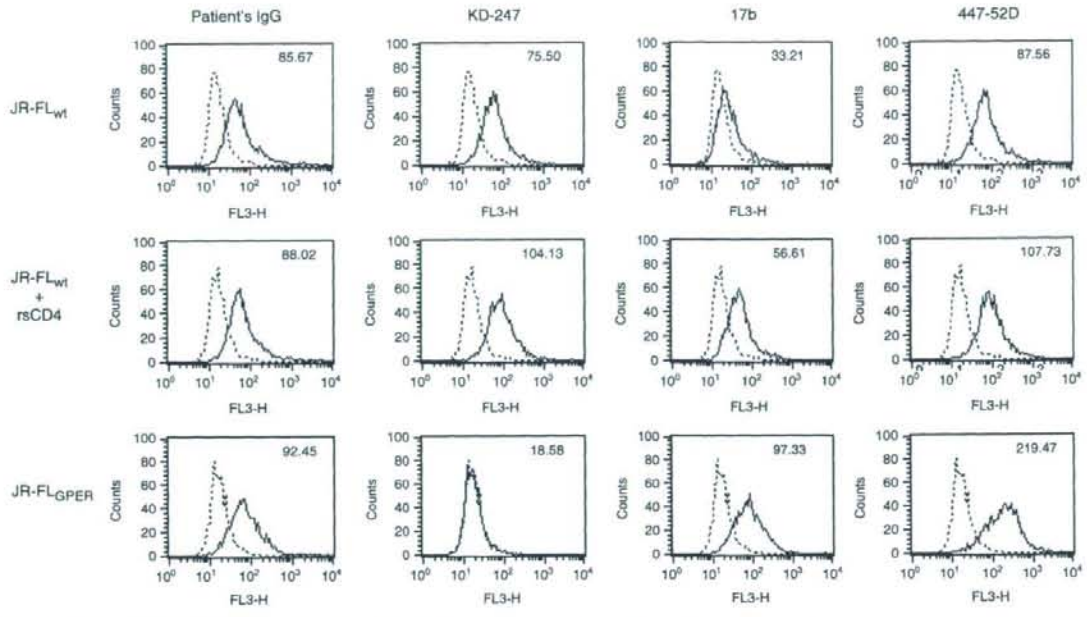

Fig. 3. Comparison of antibody binding to cell surface-expressed wild-type and GPER mutant Envs. 293T cells transfected with wild-type and GPER mutant Env-expression vectors were harvested at 36 h post-transfection and stained with the indicated antibodies. Flow cytometry data for binding of the indicated antibodies (black lines) to cell surface wild-type Env (upper), wild-type Env in the presence of 0.5 μg/ml of rsCD4 (middle) and GPER mutant Env (lower) are shown among GFP-gated 293T cells along with a control antibody (anti-human CD19; dotted lines). Data are representative of the results from at least two independent experiments. The number at the top right of each graph shows the MFI of the indicated antibodies.

interaction. Each of them binds to either CCR5 or gp120. Furthermore, our present observations suggest that the neutralizing MAb KD-247 selects an escape variant with greater sensitivity to chemokine receptor inhibitors. Based on this notion, we attempted to test the synergy of this MAb with chemokine receptor inhibitors against wild-type JR-FL.

The multiple-drug-effect analysis of Chou and colleagues [14,15] was used to analyse the effects of combinations of KD-247 with CCR5 inhibitors against JR-FL(−)8P in PM1/CCR5 cells (Table 2). As shown in Table 2, all the CI values for KD-247 with the CCR5 inhibitors (TAK-779, AK-602 or SCH-C) were < 0.5 against JR-FL(−)8P at all the inhibitory concentrations tested. In particular, the CI values for the combinations of KD-247 with SCH-C and AK-602 were less than 0.1 for IC_{90}. These results suggest that combination of KD-247 with any of the tested CCR5 inhibitors produces very highly synergistic interactions at not only high but also low inhibitory concentrations. We further evaluated the *in vitro* interactions between KD-247 and representatives of each class of currently available antiretroviral agents. Although KD-247 had favourable drug interactions with all of the agents (data not shown), the synergistic effects of KD-247 and CCR5 inhibitors were the most potent among all the combinations tested in this study.

Table 2. Combination indices (CI) for KD-247 and CCR5 inhibitors against virus JR-FL(−)8P.

CCR5 inhibitor used in combination with KD-247 (2.5–160 μg/ml)	CI values at different IC[a]		
	IC_{50}	IC_{75}	IC_{90}
AK-602 (0.3–20 nM)	0.21	0.12	0.07
TAK-779 (12.5–800 nM)	0.23	0.19	0.16
SCH-C (3–100 nM)	0.18	0.08	0.04

[a]The multiple-drug-effect analysis of Chou and colleagues was used to analyse the effects of the drugs in combination [15]. IC, Inhibitory concentration. CI < 1, synergy; 0.9 < CI < 1.1, additivity; CI > 1.1, antagonism.

Discussion

Although KD-247 shows clinical promise as a passive immunization agent for suppressing viral spread in phenotype-matched HIV-infected individuals, we also know that HIV-1 always escapes from the selection pressure of any one inhibitor by obtaining mutation(s). Therefore, we induced an HIV-1 variant that could escape from neutralization by KD-247 *in vitro* by continuously exposing the R5 virus JR-FL to increasing concentrations of KD-247 and defined the virological

properties and susceptibilities of this variant to other monoclonal antibodies (CD4i, anti-V3, anti-CD4 and anti-CCR5 MAb). The present data suggest that the KD-247 escape variant, which has a G314E mutation in the V3-tip, has not only a highly resistant phenotype against KD-247 but also greater sensitivities to CCR5 inhibitors and rsCD4, and needs higher concentration of anti-CD4 antibody for entry blocking compared with the corresponding control virus after eight passages in the absence of KD-247. These phenomena were confirmed using a pseudotyped virus containing the KD-247 escape-related G314E mutation by a single-round neutralizing assay. No previous studies have reported this G314E mutation in the V3-tip region of the R5 virus using in vitro selection by MAb. This mutation is also very rare in clinical isolates from HIV-1-infected patients [17]. Interestingly, this mutation in the V3-tip also influences the sensitivities to CCR5 inhibitors, rsCD4, anti-CD4 MAb and CD4i MAb 17b. It is not clear why KD-247 escape mutant became sensitive to rsCD4 and CCR5 inhibitors. It is conceivable that higher expression of CCR5 and CD4 on PM1/CCR5 cells may have some effect on the selection of such phenotype.

The ability to provide effective long-term antiretroviral therapy for HIV-1 infection has become a complex issue, since 40–50% of patients who initially achieve favourable viral suppression to undetectable levels subsequently experience treatment failure [18]. Moreover, a recent study reported that viruses with resistance to at least one drug were present in 1 of 10 antiretroviral-naive patients in Europe [19]. As more drug-resistant HIV-1 isolates emerge, new classes of potent antiretroviral agents targeting different steps of the HIV replicative cycle and new combinations of agents targeting different molecules, such as gp120 and CD4 or CCR5, are a welcome addition to the HIV arsenal. CCR5 inhibitors represent a new class of agents aimed at inhibiting viral entry. Following binding of gp120 to the CD4 receptor, CCR5 antagonists inhibit the interaction of gp120 with its coreceptor, an integral step in the fusion of HIV to the host cell [6–8]. As with other antiretroviral agents, resistance will likely prove to be a problem for CCR5 inhibitors [4,20]. Thus, the best strategy for preventing the occurrence of resistance is to use them in combination with other potent antiretroviral drugs. In the present study, we found that combinations of KD-247 with CCR5 inhibitors showed very strong synergistic interactions. When both antiviral reagents become available in the near future, these combinations will represent an efficient weapon against HIV-1. However, the benefit of these combinations to patients with HIV-1 infection needs to be further evaluated in clinical trials.

Taken together, the present data suggest that KD-247 has at least five advantages: (i) it exerts potent activity against a wide spectrum of subtype B HIV-1 variants, presumably due to its interaction with the IGPGR sequence in the gp120 V3 tip; (ii) viral acquisition of KD-247-resistance requires a very high concentration of KD-247 *in vitro*; (iii) at least some representatives of each class of currently available antiretroviral agents remain active against the virus variant selected *in vitro* with KD-247; (iv) the escape variant becomes more sensitive to CCR5 inhibitors and rsCD4, and is less dependent on CD4 binding for entry; and (v) combinations of KD-247 with CCR5 inhibitors show highly synergistic interactions at all inhibitory concentrations tested to date.

Acknowledgements

We thank J. Robinson for kindly providing the 17b, S. Zolla-Pazner for kindly providing the 447-52D, and Hirotomo Nakata, Kenji Maeda and Yasuhiro Kou for technical support. We also thank Yuki Azakami for excellent technical assistance.

This work was supported in part by the Ministry of Health, Labor and Welfare of Japan (H-16-AIDS-001 and -012), Grant-in-aid for Scientific Research (C-18591119) from the Ministry of Education, Science and Culture of Japan and the Cooperative Research Project on Clinical and Epidemiological Studies of Emerging and Re-emerging Infectious Diseases.

References

1. Eda Y, Takizawa M, Murakami T, Maeda H, Kimachi K, Yonemura H, *et al.* **Sequential immunization with V3 peptides from primary HIV-1 produces cross-neutralizing antibodies against primary isolates with matching narrow neutralization sequence motif.** *J Virol* 2006; **80**:5552–5562.
2. LaRosa GJ, Davide JP, Weinhold K, Waterbury JA, Profy AT, Lewis JA, *et al.* **Conserved sequence and structural elements in the HIV-1 principal neutralizing determinant.** *Science* 1990; **249**:932–935.
3. Eda Y, Murakami T, Ami Y, Nakasone T, Takizawa M, Someya K, *et al.* **Anti-V3 humanized antibody KD-247 effectively suppresses ex vivo generation of human immunodeficiency virus type 1 and affords sterile protection of monkeys against a heterologous simian/human immunodeficiency virus infection.** *J Virol* 2006; **80**:5563–5570.
4. Yusa K, Maeda Y, Fujioka A, Monde K, Harada S. **Isolation of TAK-779-resistant HIV-1 from an R5 HIV-1 GP120 V3 loop library.** *J Biol Chem* 2005; **280**:30083–30090.
5. Cecilia D, KewalRamani VN, O'Leary J, Volsky B, Nyambi P, Burda S, *et al.* **Neutralization profiles of primary human immunodeficiency virus type 1 isolates in the context of coreceptor usage.** *J Virol* 1998; **72**:6988–6996.
6. Baba M, Nishimura O, Kanzaki N, Okamoto M, Sawada H, Iizawa Y, *et al.* **A small-molecule, nonpeptide CCR5 antagonist with highly potent and selective anti-HIV-1 activity.** *Proc Natl Acad Sci USA* 1999; **96**:5698–5703.
7. Strizki JM, Xu S, Wagner NE, Wojcik L, Liu J, Hou Y, *et al.* **SCH-C (SCH 351125), an orally bioavailable, small molecule antagonist of the chemokine receptor CCR5, is a potent inhibitor of HIV-1 infection in vitro and in vivo.** *Proc Natl Acad Sci USA* 2001; **98**:12718–12723.
8. Maeda K, Nakata H, Koh Y, Miyakawa T, Ogata H, Takaoka Y, *et al.* **Spirodiketopiperazine-based CCR5 inhibitor which preserves CC-chemokine/CCR5 interactions and exerts potent activity against R5 human immunodeficiency virus type 1 in vitro.** *J Virol* 2004; **78**:8654–8662.

9. Maeda Y, Foda M, Matsushita S, Harada S. **Involvement of both the V2 and V3 regions of the CCR5-tropic human immunodeficiency virus type 1 envelope in reduced sensitivity to macrophage inflammatory protein 1alpha.** *J Virol* 2000; **74**: 1787–1793.
10. Yoshimura K, Feldman R, Kodama E, Kavlick F, Qiu YL, Zemlicka J, *et al.* **In vitro induction of human immunodeficiency virus type 1 variants resistant to phosphoralaninate prodrugs of Z-methylenecyclopropane nucleoside analogues.** *Antimicrob Agents Chemother* 1999; **43**:2479–2483.
11. Yoshimura K, Kato R, Kavlick MF, Nguyen A, Maroun V, Maeda K, *et al.* **A potent human immunodeficiency virus type 1 protease inhibitor, UIC-94003 (TMC-126), and selection of a novel (A28S) mutation in the protease active site.** *J Virol* 2002; **76**:1349–1358.
12. Hope TJ, Huang XJ, McDonald D, Parslow TG. **Steroid-receptor fusion of the human immunodeficiency virus type 1 Rev transactivator: mapping cryptic functions of the arginine-rich motif.** *Proc Natl Acad Sci USA* 1990; **87**:7787–7791.
13. Wang FX, Kimura T, Nishihara K, Yoshimura K, Koito A, Matsushita S. **Emergence of autologous neutralization-resistant variants from preexisting human immunodeficiency virus (HIV) quasi species during virus rebound in HIV type 1-infected patients undergoing highly active antiretroviral therapy.** *J Infect Dis* 2002; **185**:608–617.
14. Chou TC, Hayball MP. *CalcuSyn*. 2nd edn. Cambridge, UK: Biosoft; 1996.
15. Chou TC, Talaly P. **A simple generalized equation for the analysis of multiple inhibitions of Michaelis–Menten kinetic systems.** *J Biol Chem* 1977; **252**:6438–6442.
16. Decker JM, Bibollet-Ruche F, Wei X, Wang S, Levy DN, Wang W, *et al.* **Antigenic conservation and immunogenicity of the HIV coreceptor binding site.** *J Exp Med* 2005; **201**:1407–1419.
17. Kuiken C, Foly B, Hahn BH, Marx P, McCutchan F, Mellors J, *et al. HIV Sequence Compendium*. Los Alamos: Los Alamos National Laboratory; 2001.
18. Richman DD. **HIV chemotherapy.** *Nature* 2001; **410**:995–1001.
19. Wensing AM, van de Vijver DA, Angarano G, Asjo B, Ballota C, Boeri E, *et al.* **Prevalence of drug-resistant HIV-1 variants in untreated individuals in Europe: implications for clinical management.** *J Infect Dis* 2005; **192**:958–966.
20. Marozsan AJ, Kuhmann SE, Morgan T, Herrera C, Rivera-Troche E, Xu S, *et al.* **Generation and properties of a human immunodeficiency virus type 1 isolate resistant to the small molecule CCR5 inhibitor, SCH-417690 (SCH-D).** *Virology* 2005; **338**: 182–199.